Fermentative hydrogen production under moderate halophilic conditions

Mélanie Pierra, Eric Trably, Jean-Jacques Godon, Nicolas Bernet

Fermentative hydrogen production under moderate halophilic conditions

PIERRA Mélanie[1], TRABLY Eric[1]*, GODON Jean-Jacques[1], BERNET Nicolas[1]

[1]INRA, UR 50, Laboratoire de Biotechnologie de l'Environnement, Avenue des Etangs, 11100 Narbonne, France.

*corresponding author: eric.trably@supagro.inra.fr

Abstract

Dark fermentation is an intermediate microbial process occurring along the anaerobic biodegradation of organic matter. Saline effluents are rarely treated anaerobically since they are strongly inhibited by high salt concentrations. This study deals with the characterization of microbial communities producing hydrogen under moderate halophilic conditions. A series of batch experiments was performed under anaerobic conditions, with glucose as substrate (5 g L^{-1}) and under increasing NaCl concentrations ranging from 9 to 75 g_{NaCl} L^{-1}. A saline sediment of a lagoon collecting salt factory wastewaters was used as inoculum. Interestingly, a gradual increase of the biohydrogen production yield according to NaCl concentration was observed with the highest value (0.9 ±0.02 mol_{H2} $mol_{Glucose}^{-1}$) obtained for the highest NaCl concentration, ie. 75 g_{NaCl} L^{-1}, suggesting a natural adaptation of the sediment inoculum to salt. This work reports for the first time the ability of mixed culture to produce hydrogen in moderate halophilic environment. In addition, maximum hydrogen consumption rates decreased while NaCl concentration increased. A gradual shift of the bacterial community structure, concomitant to metabolic changes, was observed with increasing NaCl concentrations, with the emergence of bacteria belonging to *Vibrionaceae* as dominant bacteria for the highest salinities.

Key words: Biohydrogen, CE-SSCP, Dark fermentation, Pyrosequencing, Salinity, *Vibrionaceae*,

1. Introduction

The actual increasing interest in hydrogen (H_2) as a promising clean and sustainable energy carrier is mainly due to its high energy density (122 kJ g^{-1}) as well as the high efficiency of fuel cells to convert H_2 to electricity for transportation purposes [1–3]. Nowadays, most of the hydrogen produced worldwide is generated by natural gas reforming. However, producing hydrogen from fossil fuel produce more than twice carbon oxide equivalent compared to biohydrogen and contribute to resource depletion [4,5]. Developping alternatives technologies to produce hydrogen from renewable energy sources and minimizing their environmental impact are therefore of high priority. Producing hydrogen in biological processes is considered more environmentally friendly and sustainable than from conventional techniques. Particularly, dark fermentation is a process that aims at producing biohydrogen and treating organic waste at the same time [1–3,6–9]. During anaerobic digestion of those compounds, several microbial metabolism pathways outcompete for hydrogen which is a key intermediate in the trophic chain, as electron carrier (Fig. 1 – General pathways for hydrogen production. Bold arrows are represented for hydrogen production pathways, dotted arrows for hydrogen consumption pathways and dashed arrows for hydrogen production concurrent routes (adapted from Guo et al [3]).

). When applying specific operating conditions (low pH, high substrate/inoculum ratio), consumption and concurrent routes for hydrogen production can be avoided [3].

Moreover, saline wastewaters, that can be generated by fish, seafood, petroleum and leather industries, may contain large amounts of organic matter that have to be treated [10,11]. Wastewaters discharged from drinking water treatment plants using ion-exchange membrane and reverse-osmosis processes may also contain high amounts of salts [11]. Overall, saline wastewaters represent more than 5% of the worldwide effluent treatment requirements [12]. Discharging those saline wastewaters directly to the environment leads to high risks of soil, surface water and groundwater salinization. In most cases, high salinity wastewaters have to be diluted before any biological treatment to reduce their salinity. Indeed, a high salinity can disturb the osmotic balance across microbial cell walls and cause plasmolysis of microbial cells, making unefficient any biological treatment [13,14]. Dilution of saline

wastewaters implies a high increase in water consumption of the treatment bioprocess and, as a consequence, its operating costs.

Although Na^+ concentration has a strong inhibitory effect on anaerobic digestion processes [12,14,15], natural microbial communities can nevertheless well adapt to high salt concentrations to finally exhibit efficient activity for anaerobic treatment of saline wastewaters [10]. Some anaerobic microbial communities were reported as halophilic [16,17], whereas some others were non-halophilic and had to be adapted by increasing salt concentrations prior to using them as inoculum [12,18,19].

While many species from *Clostridium, Enterobacter* and *Escherichia* genera have been described in the literature as hydrogen-producing bacteria in mixed cultures in non halophilic environment [2,3,8,9,20–23], only few studies have dealt with dark fermentation of saline effluents in mixed cultures [24,25]. Regarding fermentative hydrogen production under moderate halophilic conditions with pure cultures, only *Bacillus megaterium* [26], *Halocella cellulolytica* [27] and *Clostridium acetobutylicum*[28] were reported previously to produce H_2 at pH7 and under saline conditions up to 2% w/v NaCl [26–28]. Interestingly, Alshiyab et al. [28] showed that hydrogen productivity of *Clostridium acetobutylicum* decreased by 18% while increasing NaCl concentration from 0 to 5 $g_{NaCl}\ L^{-1}$. Simankova et al. [27] reported that a halophilic bacteria, *Halocella cellulolytica,* isolated from hypersaline lagoons with high NaCl concentrations (50 to 200 $g_{NaCl}\ L^{-1}$), was also capable of hydrogen production of about 4 $mmol_{H2}\ L^{-1}$ during microcristalyne cellulose breakdown. Liu et al. [26] studied the capability of *Bacillus megaterium (Bacillus sp B2)* to produce hydrogen within a range of 4 to 70% $g_{NaCl}\ L^{-1}$. They observed a maximum hydrogen production of 1.65 $mol_{H2}\ mol_{Glucose}^{-1}$ in marine conditions (30 $g_{NaCl}\ L^{-1}$). Kivisto et al. [24] showed that *Halanaerobium saccharolyticum* sspp. *saccharolyticum* (Hssa) and *senegalensis* (Hsse) produced respectively 0.6 and 1.6 $mol_{H2}\ mol_{Glycerol}^{-1}$, at pH7 and 150 $g_{NaCl}\ L^{-1}$. Similarly, Brown et al. [29] described *Halanaerobium hydrogeniformans* as a fermentative hydrogen producer in haloalkaline conditions at pH11 and 70 $g_{NaCl}\ L^{-1}$. Those results emphasize that hydrogen producers do exist and can produce hydrogen efficiently in pure cultures under halophilic conditions, mainly in neutral or alkaline conditions unlike classical dark fermentation processes that are operated under acid conditions.

The aim of the present study is to evaluate the capability of mixed cultures to produce biohydrogen by dark fermentation under increasing NaCl concentrations. Experiments were performed in mixed culture, inoculated with a microbial ecosystem adapted to saline conditions, to provide new insights about using dark fermentation in moderate halophilic condition for producing hydrogen and treating saline waste streams at the same time, that cannot be feasible with pure cultures. A series of batch experiments was thus carried out with increasing NaCl concentrations from 9 to 75 $g.L^{-1}$ at pH 8, and using a saline sediment well adapated to halophilic conditions as inoculum.

2. Materials and Methods

2.1. Source of inoculum

The seed sediment used for hydrogen production was sampled in a lagoon collecting wastewaters from a salt factory. The sediments were filtrated through a 2 mm sieve and stored at lab temperature before inoculation. The initial pH of the sediments was 8.5 and the salinity 67.4 $g\ L^{-1}$.

2.2. Hydrogen production in batch tests

Hydrogen production experiments were performed in 600 mL glass bottles in batch conditions. About 1.5 g of the seed sediment was added to the culture medium to obtain a final concentration of 300 $mg_{VS}\ L^{-1}$ (final working volume of 200 mL). The culture medium was composed of 100mM phosphate buffer, 5 $g\ L^{-1}$ glucose and a solution oligoelements with the following final concentrations : 7.50 $g\ L^{-1}$ $FeCl_2$, H_2O, 0.30 $g\ L^{-1}$ H_3BO_3, H_2O, 0.59 $g\ L^{-1}$ $MnSO_4$, H_2O, 0.13 $g\ L^{-1}$ $CoCl_2$, $6H_2O$, 0.35g L^{-1} $ZnCl_2$, 0.13 $g\ L^{-1}$ $NiCl_2$,$6H_2O$, 0.075 $g\ L^{-1}$ $CuCl_2$,$2H_2O$, 0.13 $g\ L^{-1}$ $NaMoO_4$,$2H_2O$. The initial pH was adjusted to 8 using NaOH (1M). All batch tests were carried out in triplicate. To ensure anaerobic conditions, each bottle headspace was flushed and purged with nitrogen gas after inoculation for 5 minutes. Composition of headspace gas was checked and oxygen content was less than 0.5% in all bottles. Then, the bottles were capped with a rubber stopper and incubated at 35°C for more than 20 days. Two-milliliter aliquots were periodically collected and centrifuged (20,000g, 10 min). Supernatants and pellets were stored at -20°C. Supernatants were used for further chemical analysis and pellets for DNA extraction.

2.3. Chemical analyses

Volatile fatty acids (VFA) composition, *ie*. acetic (C2), propionic (C3), butyric and iso-butyric (C4 and iC4), valeric and iso-valeric (C5 and iC5) and caproic (C6) acids was determined with a gas chromatograph (GC-3900 Varian) equipped with a flame ionization detector. The concentrations of non-VFA metabolic products such as ethanol, lactate and formate were measured by HPLC analysis and refractometric detection, as previously described [21].

Biogas production volume was periodically estimated by measuring the gas pressure in headspace. Biogas composition (CH_4, CO_2, H_2 and N_2) was determined using a gas chromatograph (Clarus 580, Perkin Elmer) coupled to Thermal Catharometric detection (TCD), as described elsewhere [21].

2.4. Data analysis

To assess accurately H_2 production performances, cumulative H_2 production curves were fitted to a modified Gompertz equation for each batch experiment, as proposed by Quéméneur et al. [20] :

$$H_2(t) = H_{2max}.\exp(-\exp(V_{max}.\exp(1)/ H_{2max} (\lambda-t)+1))$$

where H_{2max} corresponds to the maximum experimental H_2 yield (in mol $_{H2}$ mol_{Glc}^{-1}), V_{max} : the maximum H_2 production rate (in mol_{H2} mol_{Glc}^{-1} day^{-1}), λ the lag phase (in days), and t the incubation time (in days) (see Fig. 1 – General pathways for hydrogen production. Bold arrows are represented for hydrogen production pathways, dotted arrows for hydrogen consumption pathways and dashed arrows for hydrogen production concurrent routes (adapted from Guo et al [3]).

Fig. 2).

Specific H_2 consumption rates R_c (in d^{-1}) (Fig. 12) were estimated from the H_2 decrease in cumulative H_2 values at H_{2max} time and at the end of the experiment, that was then normalized according to the corresponding H_{2max} value.

2.5. DNA extraction, PCR amplification and CE-SSCP fingerprinting

Molecular fingerprinting of the bacterial communities were performed for the samples taken at the time of maximal hydrogen production(H_{max}) for each reactor. After centrifugation (20,000g, 10 min.) of 2mL sample aliquots, genomic DNA was extracted and purified from the pellets using a PROMEGA Wizard® Genomic DNA kit. The DNA amount and purity in extracts were measured by

spectrophotometry (Infinite NanoQuant M200, Tecan). Then, 16S rRNA genes were amplified using universal primers for bacteria, named W49 (5'-ACGGTCCAGACTCCTACGGG-3' *Escherichia coli* position 330) [30] and 5'-fluorescein phosphoramidite labeled W104 (5'-6FAM-TTACCGCGGCTGCTGGCAC-3' *Escherichia coli* position 533) [30]. Each PCR (Polymerase Chain Reaction) mixture (50µL) contained 5µL of 10x Pfu Turbo DNA buffer, 200 nMf of dNTP, 500 nMf of each primer, 2.5 U μL^{-1} of Pfu Turbo DNA polymerase (Stratagene) and 10 ng of genomic DNA. Reactions were performed in Mastercycler thermal cycler (Eppendorf). The 16S rRNA genes were amplified as follows : initial denaturing at 94°C for 2 min, followed by 25 cycles performed at 94°C for 30 s, 61°C for 30 s and 72°C for 30 s, with a final elongation at 72°C for 10 min. Reactions were stopped by cooling the mixture to 4°C.

PCR products were then separated by capillary electrophoresis single-strand conformation polymorphism (CE-SSCP). This method allows the separation of DNA fragments that have about the same size but different base compositions [31]. For this, one microliter of the appropriate dilution of PCR products was mixed with 18.925 µL of formamide and 0.075 µL of internal standard GeneScan ROX (Applied Biosystems). Samples were heat-denatured at 95°C for 5 min and immediately re-cooled directly on ice for 5 min. CE-SSCP electrophoresis was performed in an ABI Prism 3130 genetic analyzer (Applied Biosystems) in 50 cm capillary tubes filled with conformation analysis polymer, corresponding buffer and 10% glycerol (Applied Biosystems). Samples were eluted at 12kV and 32°C for 30 min.

For bacterial identification, pyrosequencing of the DNA samples using a 454 protocol was performed (Research and Testing Laboratory (Lubbock, USA).

The sequences of the most abundant bacteria found for each salt concentration was deposited in the NCBI genbank database under the accession number : KC905780 for the 39% abundant bacteria at 9 $g_{NaCl}L^{-1}$, KC905779 for the 27% abundant bacteria at 9 $g_{NaCl}L^{-1}$, KC905778 for the 36% abundant bacteria at 19 $g_{NaCl}L^{-1}$, KC905777 for the 19% abundant bacteria at 29 $g_{NaCl}L^{-1}$; KC905776 for the 36% abundant bacteria at 38 $g_{NaCl}L^{-1}$; KC905775 for the 26% abundant bacteria at 38 $g_{NaCl}L^{-1}$; KC905774 for the 22% abundant bacteria at 48 $g_{NaCl}L^{-1}$; KC905773 for the 79% abundant bacteria at 58 $g_{NaCl}L^{-1}$; KC905772 for the 92% abundant bacteria at 75 $g_{NaCl}L^{-1}$.

2.6. Statistical analyses of CE-SSCP fingerprints

CE-SSCP profiles were aligned with an internal standard, ROX, to consider the inter-sample electrophoretic variability. The CE-SSCP profiles were normalized using the Statfingerprints library [32] in R software version 2.9.2 [33], with a standard procedure described by Fromin et al. [34]. The genetic distances between bacterial communities were assessed using Euclidean distances to obtain similarity matrices. Genetic distances between samples were analyzed by principal component analysis (PCA). Linear correlations between PCA ordination of bacterial communities and environmental parameters were established using the *envfit* function of the *vegan* library [35]. Average CE-SSCP profiles were calculated for each condition, and corresponded to the average abundance of individual peaks from replicates.

The Simpson diversity index was evaluated to estimate the complexity of the community by assessing the number of species (number of peaks) as well as the relative abundance (area under each peak) [36].

3. Results and Discussion

3.1. Hydrogen production performances according to NaCl concentrations

Throughout the batch experiments, no CH_4 was detected in head space, and only H_2 and CO_2 were found as gaseous products. The Gompertz model showed a good fit with the experimental H_2 production data, with determination coefficients r^2 over 0.994 for all batch tests. Fig. 3 presents the hydrogen production parameters according to NaCl concentrations. The maximum hydrogen production yield (H_{2max}) decreased from 0.65 (±0.01) $mol_{H2}\ mol_{Glucose}^{-1}$ to 0.42 (±0.02) $mol_{H2}\ mol_{Glucose}^{-1}$ when NaCl concentrations increased from 9 $g_{NaCl}\ L^{-1}$ to 19 $g_{NaCl}\ L^{-1}$. This result was consistent with previous studies that showed an inhibition of fermentative hydrogen production at low NaCl concentrations (less than 30 g_{NaCl}/L) with the same substrate (glucose) [25,28]. Alshiyab et al [28] showed that *Clostridium butylicum* presented a decrease of hydrogen productivity (18% less) from 0 to 5 $g_{NaCl}L^{-1}$ at slight lower pH and temperature conditions (pH 7, 30°C). Similarly, Zheng et al [25] showed a continuous decrease of the hydrogen production rate from 0.597 $mol_{H2}\ mol_{Sucrose}^{-1}\ d^{-1}$ to 0.089 $mol_{H2}\ mol_{Sucrose}^{-1}\ d^{-1}$ with the increase of NaCl concentration from 0 to 30 $g_{NaCl}L^{-1}$ in a more acidic medium (pH6) with heat-treated anaerobically digested sludge. In the present study, the first

loss in hydrogen production (35% for 9 to 19 g_{NaCl} L^{-1}) is consistent with these results, but the use of a not heat-treated inoculum made possible the selection of microbial populations that are halophilic tolerant, fermentative and hydrogen-producing rather than sporulating *Clostridium* strains, known to be inhibited by high NaCl concentrations.

By increasing NaCl concentration, maximum hydrogen production (H_{2max}) increased constantly up to a maximum value of 0.90 (±0.02) mol_{H2} $mol_{Glucose}^{-1}$ at 75 g_{NaCl} L^{-1}. Interestingly, this NaCl concentration (75 g L^{-1}) was very close to the natural salinity of the sediment used as inoculum (67 g L^{-1}). This suggested that the hydrogen-producing fermentative bacteria present in the inoculum were already adapted to such high NaCl concentrations.

Moreover, a decrease of the specific H_2 consumption rate was observed while increasing salinity, suggesting that hydrogen-consumers were more specifically impacted by high NaCl concentrations. Thus, the highest H_{2max} value was observed for the highest NaCl concentration (see Fig. 3). However, at NaCl concentrations above 9g_{NaCl} L^{-1}, the maximum hydrogen production rates (V_{max}) were significanlty impacted with a sharp decrease from 0.53±0.19 mol_{H2} mol_{Glc}^{-1} d^{-1} at 9g_{NaCl} L^{-1} to 0.08±0.02 mol_{H2} mol_{Glc}^{-1} d^{-1} at 19g_{NaCl} L^{-1} (Fig. 3). All batch tests were run at the same time. At 9g_{NaCl} L^{-1} hydrogen was much faster than the ones with NaCl concentration up to 19 g_{NaCl} L^{-1}. Since the exponential phase was shorter, the number of points on the curves was reduced when fitting the data to the Gompertz model: This implied a higher error on Vmax estimation by the model. The maximum hydrogen production rate obtained in this work at 9g_{NaCl} L^{-1} is in accordance with previous studies [20,23]. Indeed, Quemeneur et al. [20] obtained a maximum hydrogen production rate of 0.57±0.15 mol_{H2} mol_{Glc}^{-1} d^{-1} in similar conditions with no salt addition and using a heat-treated anaerobically-digested sludge at pH 5.5. On sucrose, Quemeneur et al. [23] showed an increase of the maximum hydrogen production rate from 0.56 mol_{H2} $mol_{Sucrose}^{-1}$ d^{-1} to 1.31 mol_{H2} $mol_{Sucrose}^{-1}$ d^{-1} due to an increase of the pH value from 4 to 6 in a non saline medium and with a heat-treated anaerobically-digested sludge.

Additionnally, by increasing NaCl concentrations, a significant increase of the lag phase was observed from 0.70 to 3.94 days (Fig. 3). A low amount of microorganisms capable of hydrogen production in the initial inoculum as well as a longer generation time of these micro-organisms could affect the lag phase. Moreover, previous studies reported an increase in lag phase due to the time for osmotic

adaptation of microorganisms to maintain their osmotic pressure through the cytoplasmic membrane [14]. Indeed, the ionic strength, determined by ions species and concentrations, is an important factor for bacteria growth [28,37]. A high level of ionic strength can result in cell lysis due to a high osmolarity environment caused by NaCl or other ions that trigger a cell dehydration through the cytoplasmic membrane [14,15]. Hydrogen producing cells have to be halotolerant or capable to adapt to salt to produce hydrogen in saline environment [14].

3.2. Shift of microbial fermentative metabolism with NaCl concentration

Fig. 4 presents the distribution of the soluble metabolites produced concomitantly with H_2. At a physiological NaCl concentration of $9g_{NaCl}\ L^{-1}$, the production of acetate and butyrate as major fermentation products suggests that *Clostridium spp* were the dominant bacteria in the mixed culture. Hydrogen production is also presented on Fig. 4. As the theoretical rate of H_2 production through the acetate and butyrate pathways is 2 moles H_2 per mole of acetate or butyrate, the experimental observation of this ratio reflects whether hydrogen is entirely produced by the acetate and butyrate pathways (value close to 2) or if H_2 is concomitantly consumed by homoacetic or other hydrogen-consuming bacteria causing an overproduction of acetate (lower than 2). Hydrogen consumption results either from homoacetogenesis producing only acetate from H_2 and CO_2 or from caproate formation from H_2 and equimolar amounts of acetate and butyrate. In Fig. 4, a clear consumption pathway is shown with no caproate production, meaning that hydrogen consumption was likely due to the activity of homoacetogenic bacteria already present in the inoculum.

Furthermore, increasing NaCl addition led to an increase of formate production, and in higher proportion above 38 gNaCl L^{-1}. The formate metabolic pathway which produces concomitantly hydrogen occurs when enteric facultative anaerobes such as *Escherichia coli* are involved [7]. However, accumulation of formate was likely due to an increase of glucose conversion to formate, and the lack in formate dehydrogenase activity or inhibition of microorganisms able to use formate for their own growth such as methanogens. Increasing salt concentration led also to an increase of the lactate concentration. Lactate pathway can be either a concurrent route for hydrogen production [38] or the result of an alternative metabolic route of hydrogen-producing bacteria under environmental stress [2]. This means that lactic bacteria were probably still active in such moderate halophilic

environment as it was previously shown by Roling et al. [39] with *Tetrogenococcus halophila* a salt-tolerant bacteria capable of mixed acif fermentation at 100 $g_{NaCl}L^{-1}$. Furthermore, ethanol production increased from 0 to 5.04 mmole between 19 and 29 gNaCl L^{-1} , respectively, and remained then stable for higher salinities. As a result, the ethanol route, which is a concurrent route of fermentative hydrogen production [2,3], was induced by highly moderate salt concentration, likely by modifying the overall metabolism of hydrogen-producing bacteria. Kivisto et al. [24] showed that halophilic bacteria *Halanaerobium saccharolyticum* (Hssa) produced low amount of ethanol by glycerol fermentation. Liu et Wang [26] showed that ethanol and acetate were the major soluble products of a pure culture of *Bacillus megaterium* from glucose in a dark fermentation process operated within a range of 4 to 70 $g_{NaCl}\,L^{-1}$. In contrast, Zheng et al. [25] showed that the ethanol fraction did not change significantly by increasing NaCl concentrations from 0 to 30 $g_{NaCl}L^{-1}$ in mixed culture with glucose as substrate.

Nevertheless, the propionate pathway seemed to be strongly inhibited by NaCl as a decrease of propionate production from 1.33 to 0.09 mmol occured from 9 to 75 $g_{NaCl}L^{-1}$, respectively. No inhibition of the hydrogen consumptionrate was observed in previous studies even though Zheng et al. [25] showed that the propionate fractions did not change significantly with NaCl concentration from 0 to 30 $g_{NaCl}L^{-1}$ in mixed culture with glucose as substrate.

3.3. Shift of the bacterial community composition towards the emergence of Vibrio subspecies as main hydrogen-producing bacteria in moderate halophilic environment

First, the 16S rRNA gene-based CE-SSCP fingerprint profiles of the cultures operated at different NaCl concentrations are presented in Fig. 5 and each profile correspond to the average of three replicates determined at the maximum H_2 production time. Overall, these profiles presented very simple communities structures with an average Simpson diversity index of 0.88±0.05, and the emergence of only one or two main peaks as main dominant bacteria for each salt concentration. A clear shift in bacterial communities was observed from 19$g_{NaCl}\,L^{-1}$ up to the highest NaCl concentration, which is consistent with the results obtained on the distribution pattern of microbial metabolites and hydrogen production performances. According to the literature dealing with fermentative hydrogen producing bacterial community [20,21], the inoculum was more diverse than

the profiles obtained within the reactors, with a Simpson diversity index of 0.98 for the inoculum bacterial community.

Fig. 6 presents the principal component analysis (PCA) comparing the genetic distances between CE-SSCP profiles representing the bacterial communities at the maximum H_2 production time, according to the experimental conditions [21]. As shown in Fig. 6, the individual profiles were highly similar under a same condition, suggesting a high reproducibility of the experiments. Moreover, samples could be clustered according to the dominant species in association with a salinity, with one group at 9 $g_{NaCl}\ L^{-1}$, one group for samples ranging from 19 to 48$g_{NaCl}\ L^{-1}$, and a last group from 58 to 75$g_{NaCl}\ L^{-1}$.These results suggested that salinity was an important factor to select different specific species in non saline conditions (cluster 1 at 9 $g_{NaCl}\ L^{-1}$), in conditions closed to marine ones (cluster 2 from 19 to 48$g_{NaCl}\ L^{-1}$) and in high halophilic conditions (cluster 3 from 58 to 75$g_{NaCl}\ L^{-1}$). Changes in lag-phase ($p<0.001$) and maximal H_2 production value (H_{2max}) ($p<0.001$) correlated significantly with the genetic distance between samples. These results show that genetic differences between bacterial communities can be directly correlated to their metabolic activity. This tendency can be observed in Fig. 4 where three distinct behaviours are clearly distinguished. In Fig.4, the cluster 1 presents acetate and butyrate production pathways and propionate consumption pathway. Cluster 2 shows additional formate production and ethanol consumption pathways. Cluster 3 presents acetate, butyrate and formate production pathways and ethanol and lactate consumption pathways with an interesting inhibition of propionate consumption pathway due to sodium chloride concentration.

One DNA sample of each triplicate was then sequenced by pyrosequencing. Table 1 presents the percentage of species representing 1% or more of the bacterial community and Fig. 7 shows the phylogenetic distribution of bacterial orders found at the maximum hydrogen . This results are in accordance with PCA results as the addition of NaCl changed substantially global bacterial community structures. Fig. 7 shows a clear shift in microbial community composition in favor of *Vibrionales* with increasing NaCl concentration. Indeed, relative abundances of *Clostridium*, *Enterobacter* and *Escherichia* species decreased as the salinity increased, and *Vibrio spp.* supplanted gradually these species (Table 1). In non-halophilic conditions, the most abundant species were

affiliated to genera *Clostridium*, *Enterobacter* and *Escherichia* ssp. In moderate halophilic conditions, *i.e.* 38 g_{NaCl} L^{-1}, bacteria belonging to *Bacteroidales* (43%) and *Vibrionales* (43%) orders were the main dominant bacteria (Fig. 7). At higher salinities, *Vibrio* spp. was the main bacteria found. The proportion of *Vibrio* spp. within the microbial community increased gradually with increasing salt concentration to reach up to 92% at 75 g_{NaCl} L^{-1}. In Cluster 3, a singular strain was identified which belongs to the family of *Vibrionaceae*. The sequence of this main strain presents a similarity percentage lower than 95% when compared to reference sequences.

Species belonging to genera *Clostridium*, *Enterobacter* and *Escherichia* are well-known as highly efficient H_2 producers, often isolated from mixed cultures able to produce hydrogen by dark fermentation in mesophilic conditions [2,3,8,9,20–23], which corroborates the results obtainedfor low saline conditions (9 g_{NaCl} L^{-1}). However, the abundance of these bacteria was significantly lower at any concentration above 9g_{NaCl} L^{-1}. This is consistent with previous reports of Alshiyab et al. [28] who studied the effect of salt addition to fermentation medium on hydrogen production. Their study was carried out at low NaCl concentrations from 0 to 5 g_{NaCl} L^{-1}. They showed that NaCl negatively impacted glucose degradation by *Clostridium acetobutylicum*, causing a productivity loss of 18% from 0 to 5 g_{NaCl} L^{-1} . Zheng et al [25] showed a decrease of 64% of H_2 yield with heat-treated anaerobic mixed cultures when increasing the salt concentration from 0 to 8.4 g_{NaCl} L^{-1}. This decrease in hydrogen yield led to similar low values of biohydrogen yield from 1.70 mol_{H2} $mol_{Glucose}^{-1}$ to 0.61 mol_{H2} $mol_{Glucose}^{-1}$ for respective NaCl concentration of 3 g_{NaCl} L^{-1} and 30 g_{NaCl} L^{-1} that is consistant with our observations of 0.65 (±0.01) mol_{H2} $mol_{Glucose}^{-1}$ at 9 g_{NaCl} L^{-1}. In contrast, at such low NaCl concentration, Lee et al. [40] showed a decrease of hydrogen production when Na^+ ion concentration increased. They studied the effect of salt concentration on metabolic pathways in dark fermentation from 0 to 12 g_{Na+} L^{-1} using an acid-treated anaerobic sludge as inoculum. . These results are not in accordance with our results, maybe because of several differences in experimental conditions. Indeed, acid pretreatment of the inoculum could have led to select spore-forming bacteria, such as members of *Clostridialesi* family, which was probably detrimental to hydrogen production at higher salt concentration, as same as our results suggested. Moreover, in our study, no pretreatment was used and

330 the inoculum originating from a saline source was used under similar conditions of salinity (for 70g_{Na+}
331 L^{-1} conditions) and pH (pH8).
332
333 Poorly referenced in the literature, hydrogen production from marine bacteria was previously observed
334 with *Bacillus megaterium* belonging to the *Bacillales* order and isolated from sludge of an intertidal
335 zone of a bathing beach in Tianjin (China) [26]. Liu et al. [26] showed that *Bacillus megaterium* could
336 be applied to biohydrogen production using both marine and fresh organic water. Best performances
337 of *Bacillus megaterium* were obtained at pH 7, 37°C and 30g_{NaCl} L^{-1} within a range of 4 and 70 g_{NaCl} L^{-1}
338 with a hydrogen production rate of 1.65 (±0.04) mol_{H2} $mol_{Glucose}^{-1}$. At salt concentration higher than
339 50 g_{NaCl} L^{-1}, Brown et al. [29] described a new alkaliphilic bacterium, *Halanaerobium*
340 *hydrogeniformans*, isolated from haloalkaline anaerobic sediments of Soap Lake in Washington State.
341 They showed that *Halanaerobium hydrogeniformans* was capable of hydrogen production in
342 haloalkaline conditions, at pH11 and 70g_{NaCl} L^{-1}. Simankova et al. [27] isolated also *Halocella*
343 *cellulolytica*, from cyanobacterials mats and anaerobic sediments of the saline lagoons of lake Sivash
344 (Crimea) of variable salinities. *Halocella cellulolytica* was able to produce hydrogen by dark
345 fermentation from a large variety of substrates, including glucose, and produces acetate, ethanol,
346 lactate, H_2 and CO_2 as fermentation products with cellulose as substrate. The optimal growth
347 parameters for this strain were pH7, 150 g_{NaCl} L^{-1}, 39 °C. *Halocella cellulolytica* produced more than
348 4 $mmol_{H2}$ L^{-1} during microcristalyne cellulose breakdown. Oh et al. [41] showed recently that five
349 *Vibrio spp*, isolated from anaerobic granular sludge, produced efficiently hydrogen with 1.22 and 1.12
350 mol_{H2} $mol_{Glucose}^{-1}$ with acetate and ethanol as main metabolites (Fig. 4). Those *Vibrio spp* presented
351 high H_2 conversion properties among 34 isolates but they were not studied under moderate halophilic
352 conditions.
353 Finally, the composition of bacterial communities at 9g_{NaCl} L^{-1} was similar to that reported in previous
354 dark fermentation studies [21–23,42,43]. Nevertheless, at 38g_{NaCl} L^{-1} *Clostridiales spp.* was in co-
355 dominance with *Vibrio spp.* Then, the bacterial community changed with increasing NaCl
356 concentration until *Vibrio spp.* became largely dominant (92%) at 75g_{NaCl} L^{-1}. At 58 g_{NaCl} L^{-1} and 75
357 g_{NaCl} L^{-1} (Cluster 3), a singular strain was identified with a percentage of identity to references

sequences lower than 95%. This strain belongs to *Vibrionaceae* and was able to produce hydrogen in high halophilic environment.

4. Conclusion

The aim of the present study was to evaluate the impact of moderate halophilic conditions on fermentative hydrogen production as well as microbial communities by increasing NaCl concentrations, with simultaneous objectives of producing biohydrogen and treating organic pollutants from saline effluents. Salt concentration presented a strong selective pressure on the structure of the bacterial communities, characterized by the emergence of a new species affiliated to the family of *Vibrionaceae. Vibrio* spp exhibited the highest hydrogen yields at the highest NaCl concentrations (0.90 ± 0.02 $mol_{H2}/mol_{Glucose}$ at 75 g_{NaCl} L^{-1}), compared to 0.65 ± 0.01 mol_{H2} $mol_{Glucose}^{-1}$ at 9 g_{NaCl} L^{-1}, likely due to lower hydrogen consumtion rates.

This work reports for the first time the ability of mixed cultures to produce biohydrogen under halophilic conditions that can be found in numerous salty waste streams that have not been used so far. Interestingly, a lowering of the hydrogen consumption rates was observed precluding of further development of efficient bioprocesses for hydrogen production with low consumption rates, and therefore higher stability. Overall, these results give new possibilities of technological development for treating saline effluents and producing biohydrogen efficiently

ACKNOWLEDGEMENTS

We gratefully acknowledge the technical and administrative supports from the "Institut National de la Recherche Agronomique" (INRA). This work was funded by the DEFIH12 Project from the French National Research Agency (ANR) (ANR contract number ANR-09-BIOE-10).

[1] Hallenbeck PC. Fermentative hydrogen production: principles, progress, and prognosis. Int J Hydrog Energy 2009;34(17):7379–7389.

[2] Hawkes F, Hussy I, Kyazze G, Dinsdale R, Hawkes D. Continuous dark fermentative hydrogen production by mesophilic microflora: principles and progress. Int J Hydrog Energy 2007;32(2):172–184.

[3] Guo XM, Trably E, Latrille E, Carrère H, Steyer J-P. Hydrogen production from agricultural waste by dark fermentation: a review. Int J Hydrog Energy 2010;35(19):10660–10673.

[4] Hajjaji N, Pons M, Renaudin V, Houas A. Comparative life cycle assessment of eight alternatives for hydrogen production from renewable and fossil feedstock. Journal of Cleaner Production 2013;44:177–189.

[5] Das D, Veziroglu TN. Hydrogen production by biological processes□ : a survey of literature. International Journal of Hydrogen Energy 2001;26:13–28.

[6] Rittmann BE. Opportunities for renewable bioenergy using microorganisms. Biotechnology and Bioengineering 2008;100(2):203–212.

[7] Hallenbeck PC, Benemann JR. Biological hydrogen production□ ; fundamentals and limiting processes. Int J Hydrog Energy 2002;27:1185–1193.

[8] Wang J, Wan W. Factors influencing fermentative hydrogen production: a review. International Journal of Hydrogen Energy 2009;34(1):799–811.

[9] Wang J, Wan W. Experimental design methods for fermentative hydrogen production: a review. International Journal of Hydrogen Energy 2009;34(1):235–244.

[10] Lefebvre O, Moletta R. Treatment of organic pollution in industrial saline wastewater: a literature review. Water Research 2006;40(20):3671–3682.

[11] Xiao Y, Roberts DJ. A review of anaerobic treatment of saline wastewater. Environmental Technology 2010;31(8-9):1025–1043.

[12] Lefebvre O, Quentin S, Torrijos M, Godon JJ, Delgenès JP, Moletta R. Impact of increasing nacl concentrations on the performance and community composition of two anaerobic reactors. Applied Microbiology and Biotechnology 2007;75(1):61–69.

[13] Vallero MVG, Hulshoff Pol LW, Lettinga G, Lens PNL. Effect of nacl on thermophilic (55 degrees c) methanol degradation in sulfate reducing granular sludge reactors. Water Research 2003;37(10):2269–2280.

[14] Oren A. The bioenergetic basis for the decrease in metabolic diversity at increasing salt concentrations: implications for the functioning of salt lake ecosystems. Hydrobiologia 2001;466(1-3):61–72.

[15] Feijoo G, Soto M, Méndez R, Lema JM. Sodium inhibition in the anaerobic digestion process: antagonism and adaptation phenomena. Enzyme and Microbial Technology 1995;17(2):180–188.

[16] Lefebvre O, Vasudevan N, Torrijos M, Thanasekaran K, Moletta R. Anaerobic digestion of tannery soak liquor with an aerobic post-treatment. Water Research 2006;40(7):1492–500.

[17] Mosquera-Corral A, Sanchez M. Simultaneous methanogenesis and denitrification of pretreated effluents from a fish canning industry. Water Research 2001;35(2):411–418.

[18] Gebauer R. Mesophilic anaerobic treatment of sludge from saline fish farm effluents with biogas production. Bioresource Technology 2004;93(2):155–67.

[19] Guerrero L, Omil F, Méndez R, Lema JM. Treatment of saline wastewaters from fish meal factories in an anaerobic filter under extreme ammonia concentrations. Bioresource Technology 1997;61(1):69–78.

[20] M. Quemeneur, J. Hamelin SB, M.T. Guidici-Orticoni , E. Latrille, JP. Steyer ET. Changes in hydrogenase genetic diversity and proteomic patterns in mixed-culture dark fermentation of mono-, di- and tri-saccharides. International Journal of Hydrogen Energy 2011;36:11654–11665.

[21] Quéméneur M, Hamelin J, Barakat A, Steyer J-P, Carrère H, Trably E. Inhibition of fermentative hydrogen production by lignocellulose-derived compounds in mixed cultures. International Journal of Hydrogen Energy 2012;37(4):3150–3159.

[22] Quéméneur M, Hamelin J, Latrille E, Steyer J-P, Trably E. Development and application of a functional ce-sscp fingerprinting method based on [fe–fe]-hydrogenase genes for monitoring hydrogen-producing clostridium in mixed cultures. International Journal of Hydrogen Energy 2010;35(24):13158–13167.

[23] Quéméneur M, Hamelin J, Latrille E, Steyer J-P, Trably E, Benomar S, Guidici-Orticoni M-T. Functional versus phylogenetic fingerprint analyses for monitoring hydrogen-producing bacterial populations in dark fermentation cultures. International Journal of Hydrogen Energy 2011;36(6):3870–3879.

[24] Kivisto A, Santala V, Karp M. Hydrogen production from glycerol using halophilic fermentative bacteria. Bioresource Technology 2010;101(22):8671–8677.

[25] Zheng XJ, Zheng YM, Yu HQ. Influence of nacl on hydrogen production from glucose by anaerobic cultures. Environmental Technology 2005;26(10):1073–80.

[26] Liu H, Wang G. Hydrogen production of a salt tolerant strain bacillus sp. b2 from marine intertidal sludge. World Journal of Microbiology & Biotechnology 2012;28(1):31–7.

[27] Simankova M, Chernych N, Osipov G, Zavarzin G. Halocella cellulolytica gen. nov., sp. nov., a new obligately anaerobic, halophilic, cellulolytic bacterium. Systematic and Applied Microbiology 1993;16:385–389.

[28] Alshiyab H, Kalil M, Hamid A, WM WY. Effect of salts addition on hydrogen production by c. acetobutylicum. Pakistan Journal of Biological Sciences 2008;(11 (18)):2193–2200.

[29] Brown SD, Begemann MB, Mormile MR, Wall JD, Han CS, Goodwin LA, Pitluck S, Land ML, Hauser LJ, Elias DA. Complete genome sequence of the haloalkaliphilic , hydrogen-producing bacterium halanaerobium hydrogeniformans 2011;193(14):3682–3683.

[30] Wéry N, Bru-Adan V, Minervini C, Delgénes J-P, Garrelly L, Godon J-J. Dynamics of legionella spp. and bacterial populations during the proliferation of l. pneumophila in a cooling tower facility. App Environ Microbiol 2008;74(10):3030–3037.

[31] Sen B, Hamelin J, Bru-Adan V, Godon J-J, Chandra TS. Structural divergence of bacterial communities from functionally similar laboratory-scale vermicomposts assessed by pcr-ce-sscp. J App Microbiol 2008;105(6):2123–32.

[32] Michelland RJ, Dejean S, Combes S, Fortun-Lamothe L, Cauquil L. Statfingerprints: a friendly graphical interface program for processing and analysis of microbial fingerprint profiles. Mol Ecol Resour 2009;9(5):1359–1363.

[33] R. Develpment Core Team. R: a language and environement for statistical computing 2010.

[34] Fromin N, Hamelin J, Tarnawski S, Roesti D, Forestier N, Gillet F, Aragno M, Rossi P. Minireview statistical analysis of denaturing gel electrophoresis (dge) fingerprinting patterns. Environ Microbiol 2007;4(2002):634–643.

[35] Oksanen J, Blanchet FG, Kindt R, Legendre P, O'Hara RB, Simpson GL, Solymos P, Stevens MHH, Wagner H. Vegan : community ecology package 2010.

[36] Simpson EH. Measurement of diversity. Nature 1949;163(4148):688.

[37] van Niel EWJ, Claassen P a M, Stams AJM. Substrate and product inhibition of hydrogen production by the extreme thermophile, caldicellulosiruptor saccharolyticus. Biotechnology and Bioengineering 2003;81(3):255–262.

[38] Noike T, Takabatake H, Mizuno O, Ohba M. Inhibition of hydrogen fermentation of organic wastes by lactic acid bacteria 2002;27:1367–1371.

[39] Roling W, Prasetyo A, Stouthamer A, Van Verseveld. Note: physiological aspects of the growth of the lactic acid bacterium tetragenococcus halophila during indonesian soy sauce (kecap) production. Journal of … 1999;06(n 19):348–352.

[40] Lee M, Kim T, Min B, Hwang S. Sodium (na+) concentration effects on metabolic pathway and estimation of atp use in dark fermentation hydrogen production through stoichiometric analysis. Journal of Environmental Management 2012;108:22–26.

[41] Oh Y-K, Park MS, Seol E-H, Lee S-J, Park S. Isolation of hydrogen-producing bacteria from granular sludge of an upflow anaerobic sludge blanket reactor. Biotechnology and Bioprocess Engineering 2003;8(1):54–57.

[42] Lin C, Chang C, Hung C. Fermentative hydrogen production from starch using natural mixed cultures. International Journal of Hydrogen Energy 2008;33(10):2445–2453.

[43] Cheng C-H, Hung C-H, Lee K-S, Liau P-Y, Liang C-M, Yang L-H, Lin P-J, Lin C-Y. Microbial community structure of a starch-feeding fermentative hydrogen production reactor operated under different incubation conditions. International Journal of Hydrogen Energy 2008;33(19):5242–5249.

Fig. 1 – General pathways for hydrogen production. Bold arrows are represented for hydrogen production pathways, dotted arrows for hydrogen consumption pathways and dashed arrows for hydrogen production concurrent routes (adapted from Guo et al [3]).

Fig. 2 – Representation of H_2 production dynamics from a mixed culture cultivated with glucose as substrate in batch. The estimated values of H_{2max}, V_{max} and Lag time correspond to the H_2 production potential (mol_{H2} mol_{Glc}^{-1}), the maximum H_2 production rate (mol_{H2} mol_{Glc}^{-1} day^{-1}) and the lag phase time (day), respectively. The Rc value corresponds to the H_2 consumption rate and was estimated by the H_2 decrease measured experimentally between the H_{2max} time and the end of the experiments, and then normalized according to H_{2max} value.

Fig. 3 - Hydrogen production parameters of the modified Gompertz model according to NaCl concentrations. (a) maximum hydrogen production rate, (b) hydrogen production yield and (c) lag phase (d) H_2 consumption rate.

Fig. 4 - Metabolic end-product distribution (in mmoles) and maximal H2 production (in mmoles) according to NaCl concentrations. The values correspond to the average of three replicates

Fig. 5 - CE-SSCP profiles based on 16S rRNA gene fragments retrieved from H_2-producing mixed cultures supplemented with different NaCl concentration. The profiles correspond to samples taken at the maximum H_2 production time. The X and Y axes of each peak represent respectively the relative peak electrophoresis migration distance and the relative peak intensity (Arbitrary Units).

Fig. 6 - Principal Component Analysis (PCA) biplot of CE-SSCP profiles. For each salinity, triplicates were clustered with ovals. The first two principal components (Axis1 and Axis2) explained 69,6% of the genetic variation. Significant linear correlations between changes in genetic profiles and changes in environment parameters are indicated by arrows: lag phase ($p<0,001$), salinity ($p<0,001$) and H2max ($p<0,001$).

Fig. 7 - Phylogenetic distribution of bacterial orders found at the maximum hydrogen production time and for different NaCl concentrations.

Table 1 - Taxonomic classification of bacterial taxonomic distribution (in %) according to the salt concentration, and obtained by pyrosequencing. Bacterial orders are presented in boldcase while species or closest known phylogenetical level in italics. Names in italics correspond to the closest physiogenetical known sequence depending on the percentage of identity (I) to reference sequence (species if $I > 97\%$; genus if $97\% \geq I > 95\%$; family if $95\% \geq I > 90\%$; order if $90\% \geq I > 85\%$). Relative abundance was defined as the number of sequences affiliated with that taxon divided by the total number of sequences per sample. Phyla, classes, and genera making up less than 1% of total composition in all libraries were grouped as “others”.

Table

Table 1

% **ORDER** / *species (closest physiogenetical known sequence)*	$9g_{NaCl}$/L	19gNaCl/L	29gNaCl/L	38gNaCl/L	48gNaCl/L	58gNaCl/L	75gNaCl/L
ALTEROMONADALES	**1**	**19**	**6**	**2**	**1**	**0**	**0**
Pseudoalteromonas sp	1	19	6	2	1	0	0
BACTEROIDALES	**0**	**0**	**19**	**5**	**26**	**16**	**2**
Bacteroidaceae (unk genus)	0	0	1	0	4	0	0
Bacteroidales (unk family)	0	0	16	4	19	15	2
Porphyromonadaceae (unk genus)	0	0	2	1	3	1	0
CLOSTRIDIALES	**44**	**28**	**29**	**43**	**17**	**2**	**2**
Clostridiaceae (unk genus)	4	9	14	1	0	2	2
Clostridiaceae unclassified (unk genus)	0	0	1	**36**	0	0	0
Clostridiales (unk family)	0	0	1	6	0	0	0
Clostridium (unk species)	**39**	1	0	0	0	0	0
Clostridium cochlearium	0	1	1	0	0	0	0
Clostridium sp	1	0	0	0	0	0	0
Clostridium thiosulfatireducens	0	5	1	0	0	0	0
Oscillibacter valericigenes	0	12	11	0	17	0	0
ENTEROBACTERIALES	**47**	**2**	**0**	**0**	**0**	**0**	**0**
Enterobacter hormaechei	4	0	0	0	0	0	0
Enterobacter sp	27	1	0	0	0	0	0
Escherichia (unk species)	1	0	0	0	0	0	0
Escherichia coli	8	0	0	0	0	0	0
Escherichia sp	7	1	0	0	0	0	0
FUSOBACTERIALES	**0**	**0**	**1**	**0**	**0**	**0**	**0**
Propionigenium maris	0	0	1	0	0	0	0
VIBRIONALES	**3**	**47**	**38**	**43**	**47**	**79**	**92**
Vibrio nereis	0	0	13	**26**	**22**	0	0
Vibrio parahaemolyticus	1	11	4	1	0	0	0
Vibrio proteolyticus	0	0	1	0	0	0	0
Vibrio sp	2	**36**	**19**	16	17	0	0
Vibrio tubiashii	0	0	1	0	0	0	0
Vibrionaceae (unk genus)	0	0	0	0	8	**79**	**92**
Others	**5**	**4**	**7**	**7**	**9**	**3**	**4**

Figure

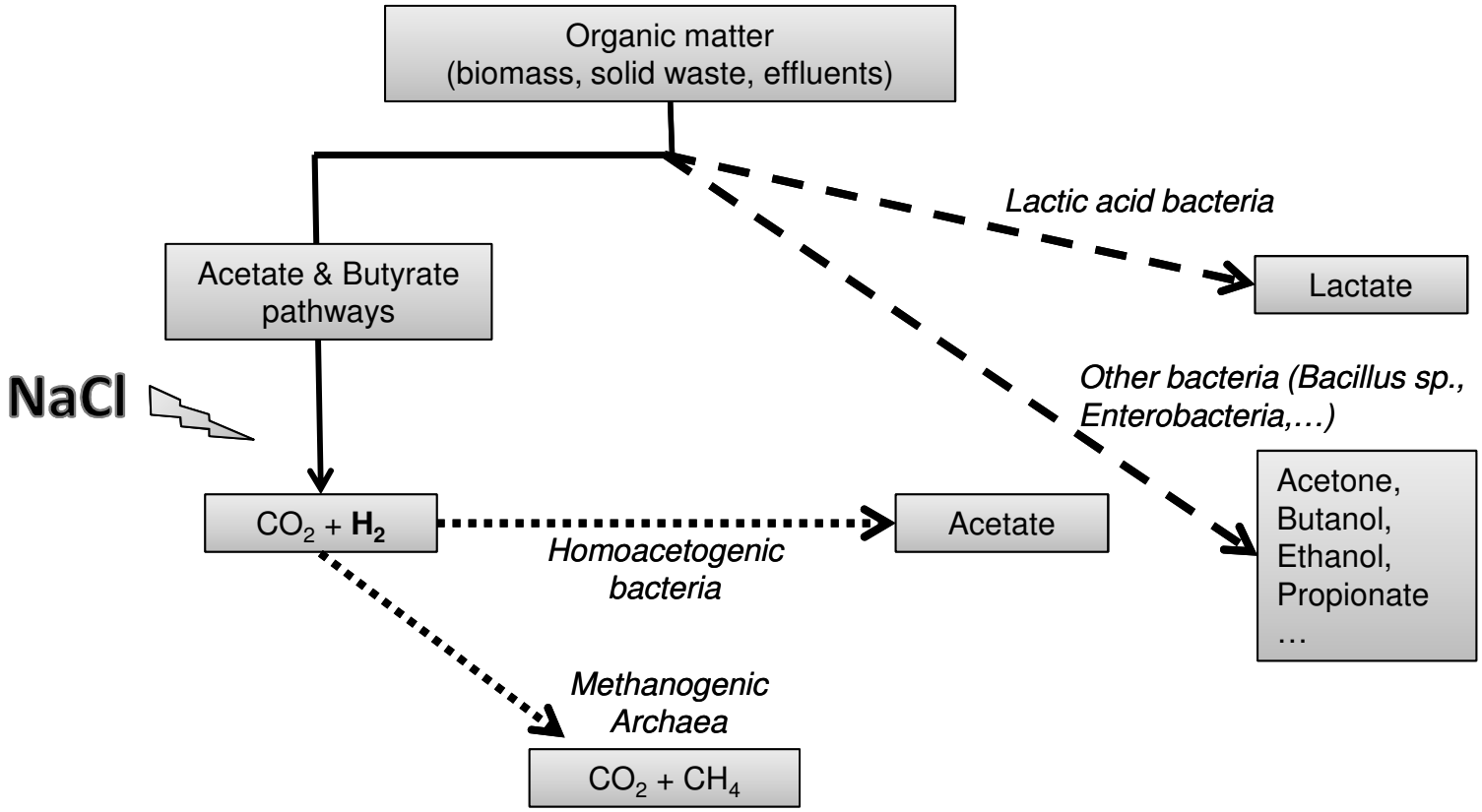
Organic matter
(biomass, solid waste, effluents)
Acetate & Butyrate
pathways
NaCl
CO_2 + H_2
Homoacetogenic
bacteria
Acetate
Methanogenic
Archaea
CO_2 + CH_4
Lactic acid bacteria
Lactate
Other bacteria (Bacillus sp.,
Enterobacteria,…)
Acetone,
Butanol,
Ethanol,
Propionate
…

Figure

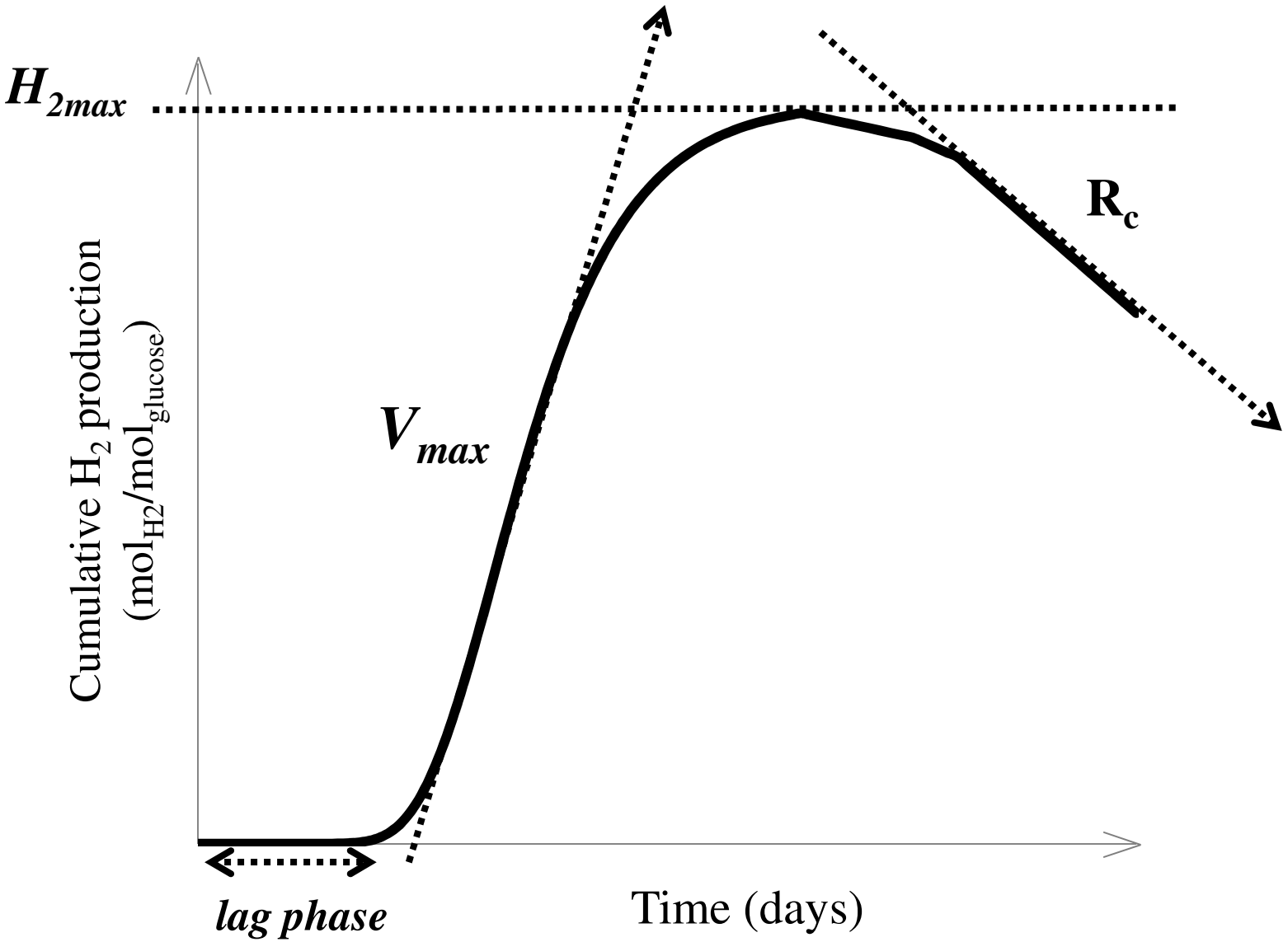
H_{2max}
V_{max}
R_c
Cumulative H_2 production
($mol_{H2}/mol_{glucose}$)
lag phase
Time (days)

Figure

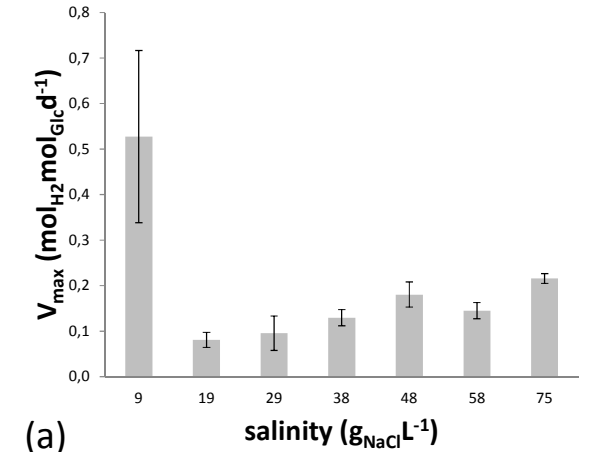
0,8
0,7
0,6
0,5
0,4
0,3
0,2
0,1
0,0
V_{max} ($mol_{H2}mol_{Glc}d^{-1}$)
9
19
29
38
48
58
75
salinity ($g_{NaCl}L^{-1}$)

(a)

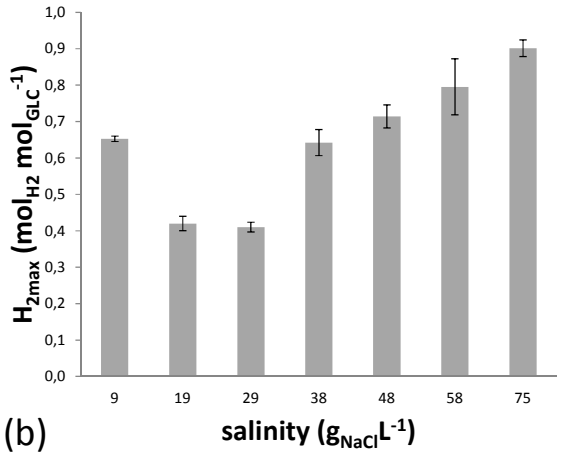
1,0
0,9
0,8
0,7
0,6
0,5
0,4
0,3
0,2
0,1
0,0
H_{2max} (mol_{H2} mol_{GLC}^{-1})
9
19
29
38
48
58
75
salinity ($g_{NaCl}L^{-1}$)

(b)

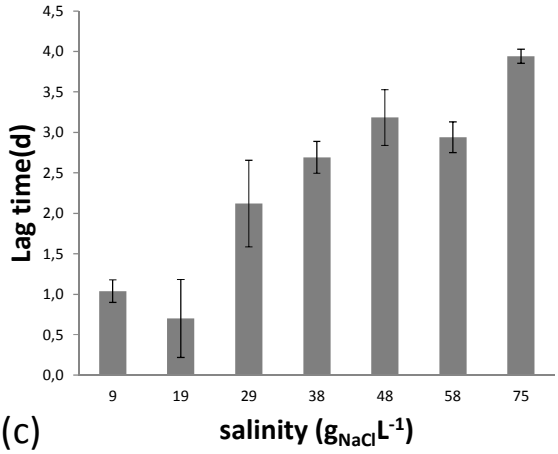
4,5
4,0
3,5
3,0
2,5
2,0
1,5
1,0
0,5
0,0
Lag time(d)
9
19
29
38
48
58
75
salinity ($g_{NaCl}L^{-1}$)

(c)

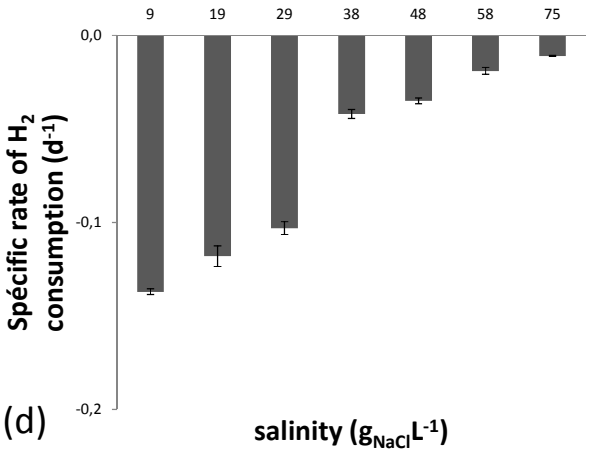
9
19
29
38
48
58
75
0,0
-0,1
-0,2
Spécific rate of H_2 consumption (d^{-1})
salinity ($g_{NaCl}L^{-1}$)

(d)

Figure

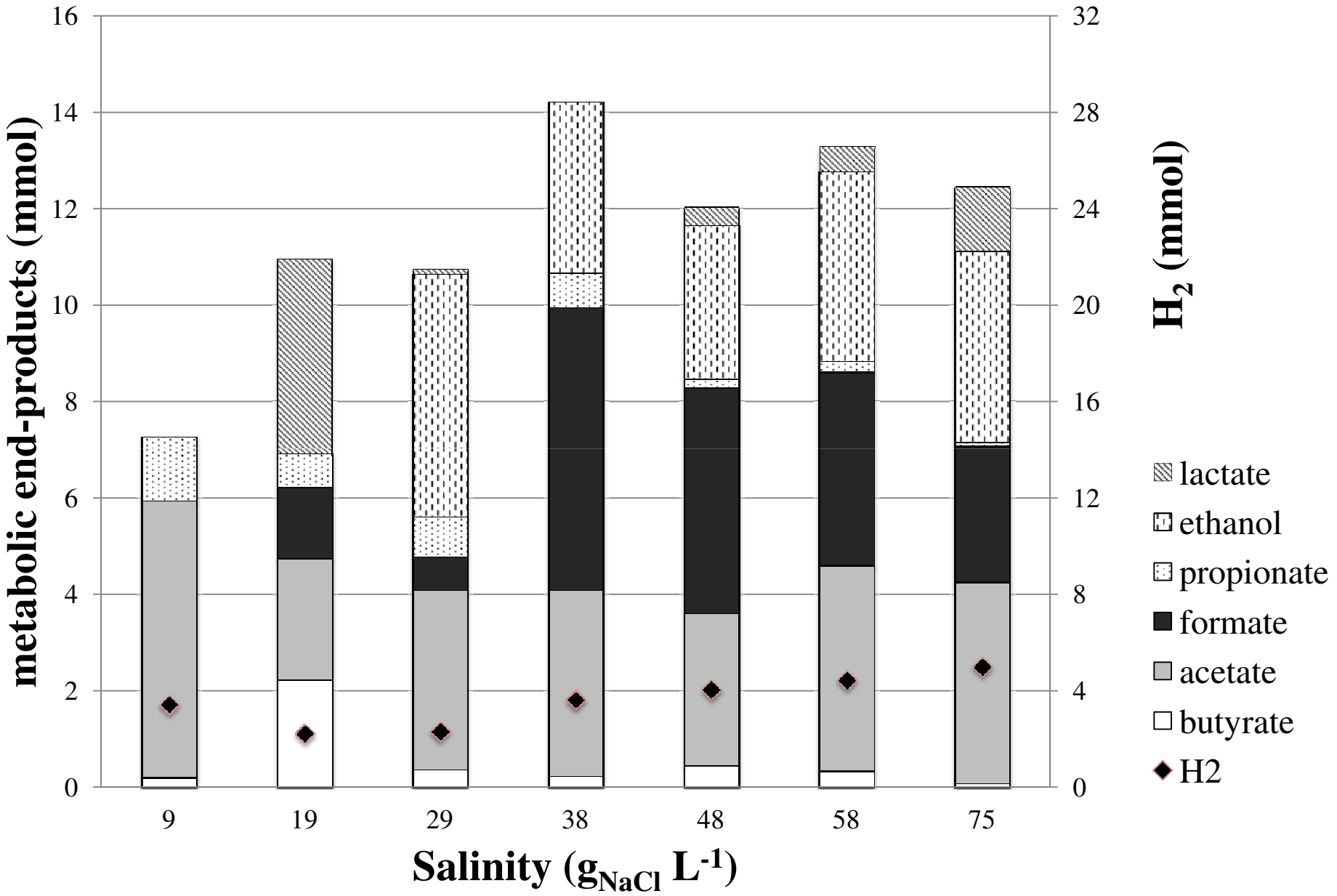
metabolic end-products (mmol)
H_2 (mmol)
Salinity (g_{NaCl} L^{-1})
0
2
4
6
8
10
12
14
16
0
4
8
12
16
20
24
28
32
9
19
29
38
48
58
75
lactate
ethanol
propionate
formate
acetate
butyrate
H2

Figure

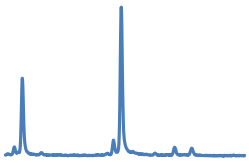

9 $g_{NaCl}L^{-1}$

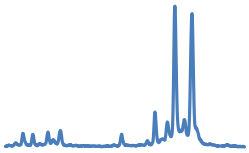

19 $g_{NaCl}L^{-1}$

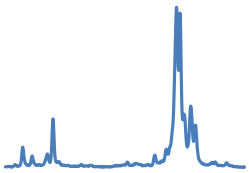

29 $g_{NaCl}L^{-1}$

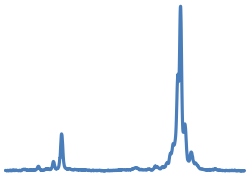

38 $g_{NaCl}L^{-1}$

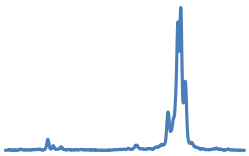

48 $g_{NaCl}L^{-1}$

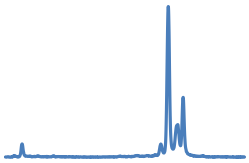

58 $g_{NaCl}L^{-1}$

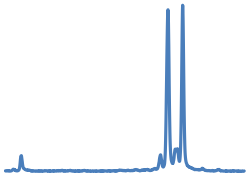

75 $g_{NaCl}L^{-1}$

Figure

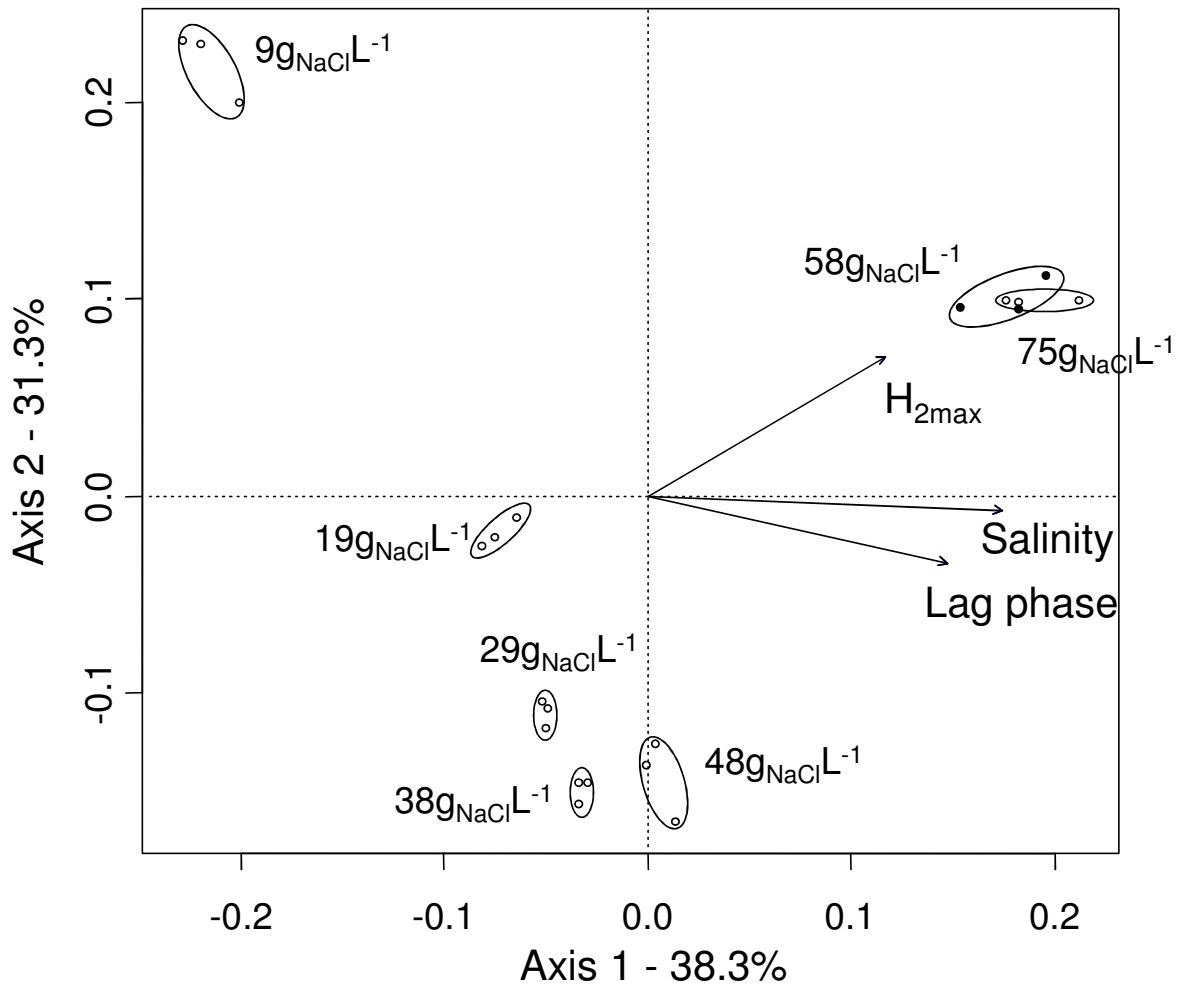
9g$_{NaCl}$L^{-1}
58g$_{NaCl}$L^{-1}
75g$_{NaCl}$L^{-1}
H$_{2max}$
19g$_{NaCl}$L^{-1}
Salinity
Lag phase
29g$_{NaCl}$L^{-1}
48g$_{NaCl}$L^{-1}
38g$_{NaCl}$L^{-1}
Axis 2 - 31.3%
0.2
0.1
0.0
-0.1
-0.2
-0.1
0.0
0.1
0.2
Axis 1 - 38.3%

Figure

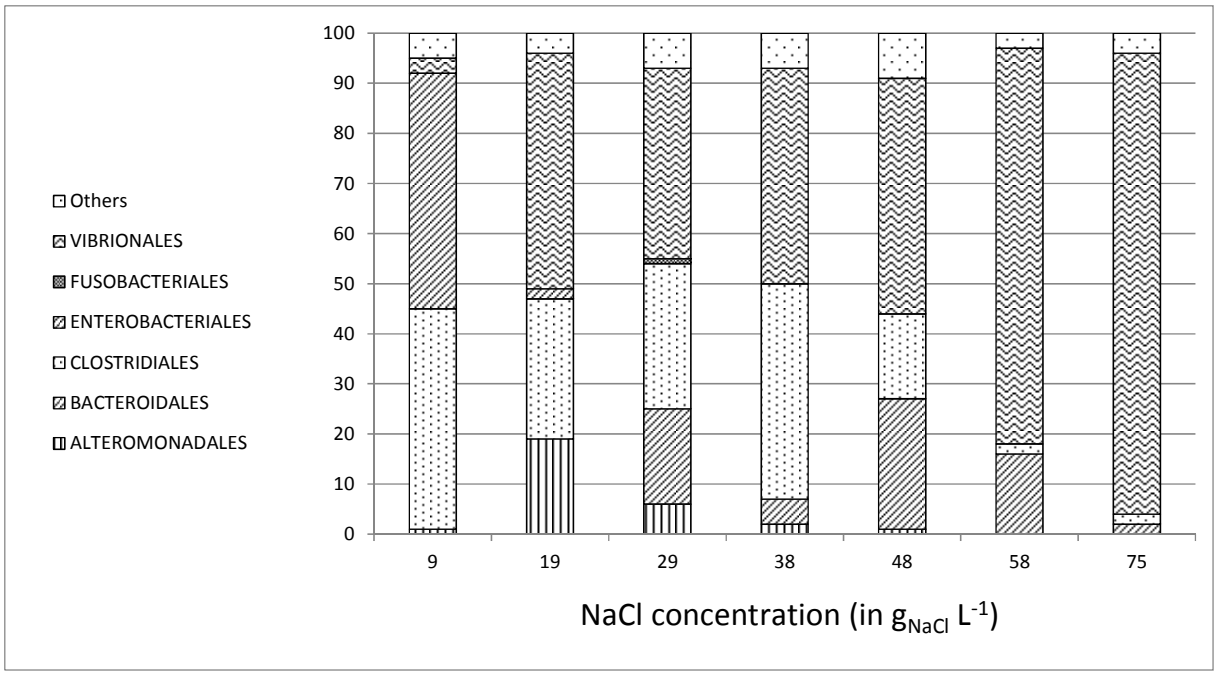
Others
VIBRIONALES
FUSOBACTERIALES
ENTEROBACTERIALES
CLOSTRIDIALES
BACTEROIDALES
ALTEROMONADALES
100
90
80
70
60
50
40
30
20
10
0
9
19
29
38
48
58
75
NaCl concentration (in g_{NaCl} L^{-1})